CHINESE OPTICS LETTERS

Vol. 19, No. 5 | May 2021

Pattern-adaptive error diffusion algorithm for improved phase-only hologram generation

Kexuan Liu (刘珂瑄), Zehao He (何泽浩), and Liangcai Cao (曹良才)*

State Key Laboratory of Precision Measurement Technology and Instrument, Department of Precision Instrument, Tsinghua University, Beijing 100084, China

*Corresponding author: clc@tsinghua.edu.cn

Received October 1, 2020 | Accepted October 19, 2020 | Posted Online February 8, 2021

The bidirectional error diffusion (BERD) algorithm is free from random phase modulation that introduces speckle noise on the reconstructed images, compared with other computer-generated phase-only hologram (POH) approaches. During the POH generation process, the amplitudes of all pixels are traditionally set to one for diffusing the errors to their neighborhood of unprocessed pixels. In this paper, we reveal that the reconstruction quality depends on the uniform amplitude value for different object pattern. The pattern-adaptive BERD (PA-BERD) algorithm is proposed for high-quality holographic reconstruction. The optimized amplitude value can be acquired for each object pattern and each propagation distance. The PA-BERD-based POHs have shown higher reconstruction quality than traditional BERD-based POHs in simulations as well as optical experiments.

Keywords: holography; computer holography; holographic display.
DOI: 10.3788/COL202119.050501

1. Introduction

The computer-generated hologram (CGH), as a promising technology for three-dimensional display, has attracted broad attention in the past two decades[1–4]. Since no display device can modulate the amplitude and phase of the incident light field simultaneously, the complex amplitude hologram (CAH) needs to be converted to an amplitude hologram or a phase-only hologram (POH) for display. Compared with the amplitude hologram, the POH provides higher diffraction efficiency and avoids the twin image in the reconstruction. The approaches to obtain POHs include the Gerchberg–Saxton algorithm[5–7], the one-step phase retrieval method[8], the bidirectional error diffusion (BERD) method[9–12], and so on. Different from other approaches, no random phase is added in the CAH generation process with the BERD method. Therefore, the influence of speckle noise on the reconstructed images is effectively eliminated, which significantly improves the image quality.

The concept of error diffusion was first proposed for halftone image generation in 1976[13] and applied to the generation of the CGH in 1984[14]. Due to the limitation of the display devices at that time, the error diffusion method was initially applied to convert the CGH into a binary hologram. The follow-up studies were mainly about the optimization of four weighting coefficients in the error diffusion process[15,16]. With the development of electronic display technology, spatial light modulators (SLMs) have replaced films as common display devices for CGHs. In 2013, the application of the error diffusion method in the conversion of the CAH to the POH was proposed[17]. This algorithm eliminates the need for random phase and iteration, significantly reducing the calculation time. Its reconstructed images are very similar to those obtained with the original complex holograms. In 2014, parallel computation and low-pass filtering were proposed to decrease the calculation time by over two orders of magnitude[18]. In 2019, four weighting parameters were modified for different holograms by using the genetic algorithm[19].

In the POH generation process with the traditional BERD method, the amplitudes of all pixels are traditionally set to one, and the corresponding errors are diffused to their neighborhood of unprocessed pixels to compensate for the discarded amplitude information. However, different CAHs have different amplitude distributions. The uniform amplitude value of one is not suitable for all images. There is still obvious coding noise on the reconstructed images of some object patterns with the BERD algorithm. In this paper, an optimization algorithm called the pattern-adaptive BERD (PA-BERD) algorithm is proposed. An optimized uniform amplitude value in the error calculation process is chosen for each object pattern and each propagation distance, which effectively eliminates the coding noise and generally improves the reconstruction quality.

2. Method

Figure 1 shows the processing procedure of the POH generation with the error diffusion method. The wave propagation from the object plane to the hologram plane is described by the angular-spectrum method[20]. No paraxial approximation is added in the calculation process, so the diffraction result is more accurate. The CAH is given by

$$H(x,y) = F^{-1}\{F\{I_O(x,y)\}H_F(f_x f_y)\}, \tag{1}$$

where $I_O(x,y)$ denotes the intensity of the object image, $H_F(f_x,f_y)$ denotes the angular-spectrum transfer function, and F and F^{-1} denote the Fourier transform and inverse Fourier transform, respectively. The transfer function from the object plane to the hologram plane is given by

$$H_F(f_x,f_y) = \exp\left(ikz\sqrt{1-\lambda^2 f_x^2-\lambda^2 f_y^2}\right), \tag{2}$$

where $k = 2\pi/\lambda$, λ is the wavelength of the optical beam, z denotes the propagation distance, and (f_x,f_y) denote the spatial frequencies. To avoid the circular convolution, the object image should be padded with zeros to twice the original size. The calculated CAH is composed of the amplitude component and phase component, as shown in Fig. 1(a).

Thereafter, the CAH is converted into the POH $H_P(x,y)$ by using the error diffusion method. First, the amplitude distribution of the complex hologram is normalized. Then, each pixel is scanned sequentially, and its amplitude value is set to one to generate the POH $H_P(x,y)$, as given by

$$H(x_j,y_j) = A(x_j,y_j)\exp[i\varphi(x_j,y_j)], \tag{3}$$

$$H_P(x_j,y_j) = \exp[i\varphi(x_j,y_j)]. \tag{4}$$

The corresponding error is given by

$$E(x_j,y_j) = H(x_j,y_j) - H_P(x_j,y_j) = [A(x_j,y_j)-1]\exp[i\varphi(x_j,y_j)]. \tag{5}$$

It is noteworthy that the complex value $H(x_j,y_j)$ of each pixel (x_j,y_j) is constantly updated in the error diffusion process, so the $H(x_j,y_j)$ used in Eq. (3) is the complex value after being diffused by the neighborhood processed pixels.

It is shown that the error between the complex value and the pure phase value is directly related to the discarded amplitude information $A(x_j,y_j)$. The error diffusion algorithm encodes the discarded amplitude information into the phase component $\exp[i\varphi(x_j,y_j)]$ by introducing the error term. It can keep the reconstruction quality of the POH similar to that of the CAH. However, the amplitude $A(x,y)$ has its own distribution according to the original object pattern and diffraction parameters. Its average value may be near to one or far below one. It is closely related to the degree of the amplitude component encoded to the phase component. As we shall show later, the reconstructed images of some objects are accompanied with obvious coding noise. In this work, we propose an algorithm to adjust the uniform amplitude value in the error calculation process for different object patterns, known as the PA-BERD algorithm. A variable parameter α is introduced to replace the value of one. The error used in the PA-BERD calculation process is given by

$$\begin{aligned} E_\alpha(x_j,y_j) &= H(x_j,y_j) - \alpha H_P(x_j,y_j) \\ &= [A(x_j,y_j)-\alpha]\exp[i\varphi(x_j,y_j)]. \end{aligned} \tag{6}$$

Thus, we can adjust the degree of the amplitude component encoded to the phase component by changing the value of α.

As shown in Fig. 1(b), the pixels on odd rows are scanned from left to right, and their errors are diffused to the neighborhood pixels as follows:

$$H(x_j,y_j+1) \leftarrow H(x_j,y_j+1) + w_1 E_\alpha(x_j,y_j), \tag{7}$$

$$H(x_j+1,y_j-1) \leftarrow H(x_j+1,y_j-1) + w_2 E_\alpha(x_j,y_j), \tag{8}$$

$$H(x_j+1,y_j) \leftarrow H(x_j+1,y_j) + w_3 E_\alpha(x_j,y_j), \tag{9}$$

$$H(x_j+1,y_j+1) \leftarrow H(x_j+1,y_j+1) + w_4 E_\alpha(x_j,y_j), \tag{10}$$

where w_1 to w_4 are the Floyd–Steinberg coefficients ($w_1 = 7/16$, $w_2 = 3/16$, $w_3 = 5/16$, and $w_4 = 1/16$). As shown in Fig. 1(c),

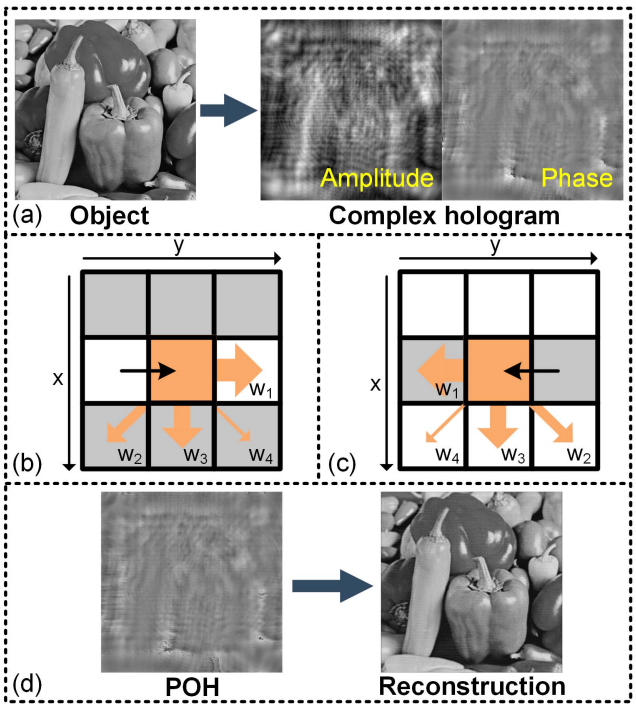

Fig. 1. Processing procedure of POH with the error diffusion method. (a) Object and its CAH. (b) The error diffusion mode for odd rows, and black arrow denotes the scanning direction. (c) The error diffusion mode for even rows. (d) The calculated POH and its reconstruction.

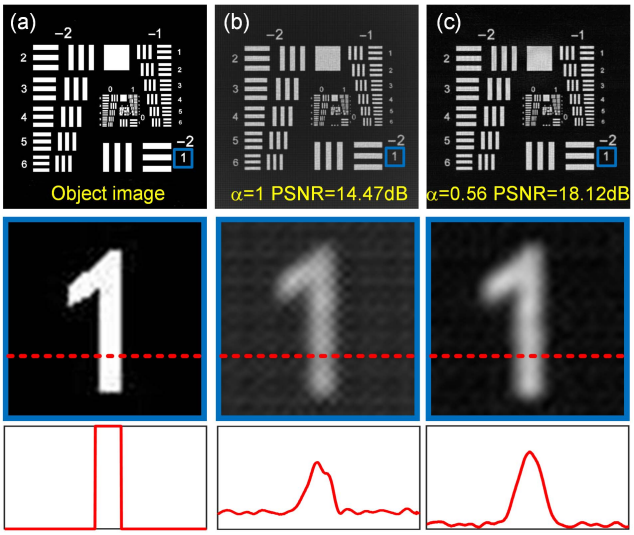

Fig. 2. Numerical reconstructions of the resolution test chart using different methods. (a) Object image. (b) Numerical reconstruction with the BERD algorithm. (c) Numerical reconstruction with the proposed PA-BERD algorithm.

the pixels on even rows are scanned from right to left, and their errors are diffused to the neighborhood pixels as follows:

$$H(x_j,y_j-1)\leftarrow H(x_j,y_j-1)+w_1E_\alpha(x_j,y_j), \tag{11}$$

$$H(x_j+1,y_j+1)\leftarrow H(x_j+1,y_j+1)+w_2E_\alpha(x_j,y_j), \tag{12}$$

$$H(x_j+1,y_j)\leftarrow H(x_j+1,y_j)+w_3E_\alpha(x_j,y_j), \tag{13}$$

$$H(x_j+1,y_j-1)\leftarrow H(x_j+1,y_j-1)+w_4E_\alpha(x_j,y_j). \tag{14}$$

As shown in Fig. 1(d), the POH generated with the PA-BERD algorithm can be reconstructed by the inverse angular-spectrum propagation, as given by

$$I(x,y)=F^{-1}\left\{\frac{F\{H_P(x,y)\}}{H_F(f_x,f_y)}\right\}. \tag{15}$$

For each object pattern, α is set from 0 to 1.5 with the interval of 0.01. The best value is acquired according to the reconstruction quality by using peak signal-to-noise ratio (PSNR) as the evaluation standard. It is shown that the best value of α is different for each object pattern because of the amplitude distribution $A(x,y)$. In this work, we calculate the optimized α for different patterns at different propagation distances.

3. Experiments

The resolution test chart is used to evaluate the proposed method. The image size is 512×512 pixels. The hologram size is 1024×1024 pixels, and the pixel pitch is 3.74 μm. The wavelength is 532 nm, and the distance between the object plane and the hologram plane is 60 mm. The CAH is calculated by the angular-spectrum method. The CAH is converted into POHs with the original BERD algorithm and the proposed PA-BERD algorithm, respectively. The reconstructed results are shown in Fig. 2. With the optimized uniform amplitude $\alpha=0.56$, the coding noise in the reconstructed image introduced by the original BERD algorithm is removed, and the PSNR of the reconstructed image is improved by 3.65 dB.

Numerical simulations of some standard test images with the original BERD algorithm and the proposed PA-BERD algorithm are also taken. The PSNR improvements of the corresponding reconstructed images are shown in Fig. 3. It is obvious that the proposed PA-BERD algorithm can generally improve the reconstruction quality, which proves its universal applicability. The improvements vary from image to image, and the highest one is 3.59 dB.

To illustrate the reconstruction quality for different values of α, the PSNR-α curve is shown in Fig. 4. With the increase of α, the PSNR first rises and then oscillates sharply and drops. By observing the reconstructed images, the rising area corresponds to the filling process of low-frequency information, and the reconstructed image information is incomplete. The oscillating area corresponds to the reconstructed images with complete information and different degrees of coding noise. The parameter $\alpha=1$ used in the traditional BERD algorithm is in this area.

Compared with the random phase method, the propagation range where the object can be clearly reconstructed by the BERD method is narrow. Figure 5 shows the reconstructed images at different propagation distances by the BERD algorithm. Diffusely extended noise clouds exist in the reconstructed

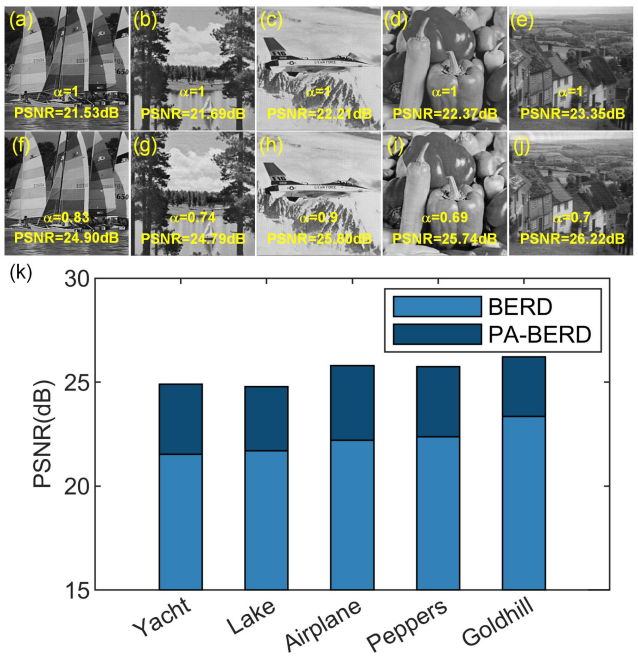

Fig. 3. Reconstruction quality improvement of different object images by the PA-BERD algorithm. (a)–(e) are the reconstructed images with the BERD algorithm. (f)–(j) are the reconstructed images with the proposed PA-BERD algorithm. (k) is the PSNR comparison of (a)–(j).

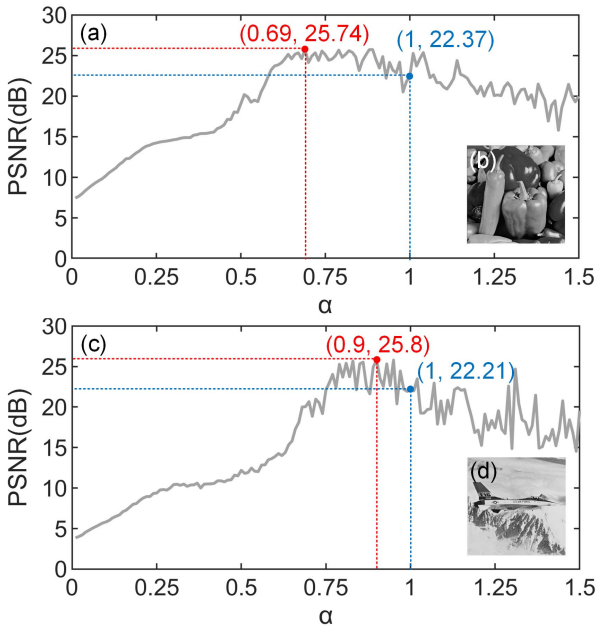

Fig. 4. (a) and (c) show the relationship between the value of α and the PSNR of the reconstructed images of (b) "Peppers" and (d) "Airplane", respectively. The blue and red dots represent the simulation results of the BERD algorithm and the PA-BERD algorithm, respectively.

images at 40 mm, 70 mm, and 80 mm, respectively. In contrast, the proposed PA-BERD algorithm can effectively eliminate the noise. The wider display distance range has opened the possibility to apply the error diffusion method in three-dimensional holographic display.

The experimental setup is shown in Fig. 6. A Holoeye Gaya SLM with the resolution of 3840×2160 pixels and the pixel

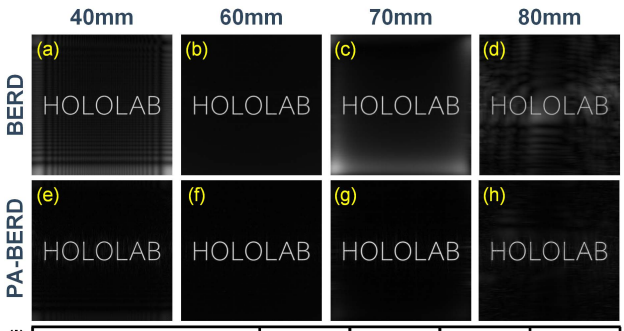

(i)

		40mm	60mm	70mm	80mm
BERD	α	1	1	1	1
	PSNR(dB)	17.35	24.45	20.76	18.84
PA-BERD	α	0.36	0.58	0.47	0.38
	PSNR(dB)	23.63	26.44	26.14	23.36

Fig. 5. Numerical reconstructions at different distances using different methods. (a)–(d) are the reconstructed images with the BERD algorithm at the distances of 40, 60, 70, and 80 mm, respectively. (e)–(h) are the reconstructed images with the proposed PA-BERD algorithm at the distances of 40, 60, 70, and 80 mm, respectively. (i) is the PSNR comparison of (a)–(h).

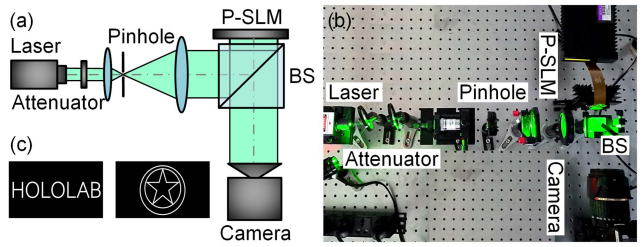

Fig. 6. (a) and (b) are the schematic and photograph of the experimental setup, respectively. (c) shows the object image patterns "HOLOLAB" and "star".

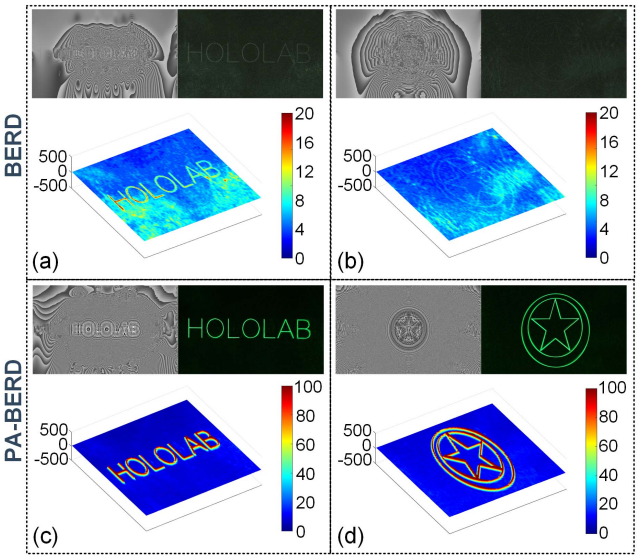

Fig. 7. Optical reconstruction results using different methods. (a) and (b) are the POHs and the corresponding optical reconstructed images and intensity distributions of "HOLOLAB" and "star" using the BERD algorithm, respectively. (c) and (d) are the POHs and the corresponding optical reconstructed images and intensity distributions of "HOLOLAB" and "star" by using the proposed PA-BERD algorithm, respectively.

pitch of 3.74 μm was used to modulate the phase of the incident laser. By adding offset phase to the holograms in the experiment, the noise caused by the SLM itself was removed. Improved reconstructed results with reduced noise were obtained.

The experimental results are shown in Fig. 7. It can be observed that the images reconstructed by the original BERD method are dark with much coding noise. However, the proposed PA-BERD algorithm can effectively improve the contrast and remove the coding noise. It is shown that the PA-BERD algorithm could support higher-quality reconstruction over the traditional BERD algorithm.

4. Conclusion

In summary, this paper reports an optimization algorithm for POH generation based on the PA-BERD method. The optimized amplitude value of α is introduced in the error calculation

process for each object pattern and each propagation distance, which effectively eliminates the coding noise and improves the reconstruction quality. The PA-BERD algorithm could be applied to POHs based on the phase plate, phase-only liquid crystal (LC)-SLM, or phase-only metasurfaces.

Acknowledgement

This work was supported by the National Natural Science Foundation of China (NSFC) (Nos. 61827825 and 61775117), the Tsinghua University Initiative Scientific Research Program (No. 20193080075), and the Cambridge Tsinghua Joint Research Initiative.

References

1. Z. He, X. Sui, G. Jin, and L. Cao, "Progress in virtual reality and augmented reality based on holographic display," Appl. Opt. **58**, A74 (2019).
2. Q. Ma, L. Cao, Z. He, and S. Zhang, "Progress of three-dimensional light-field display [Invited]," Chin. Opt. Lett. **17**, 111001 (2019).
3. Y. Zhang, J. Liu, X. Li, and Y. Wang, "Fast processing method to generate gigabyte computer generated holography for three-dimensional dynamic holographic display," Chin. Opt. Lett. **14**, 030901 (2016).
4. Y. Zhao, L. Cao, H. Zhang, W. Tan, S. Wu, Z. Wang, Q. Yang, and G. Jin, "Time-division multiplexing holographic display using angular-spectrum layer-oriented method (Invited Paper)," Chin. Opt. Lett. **14**, 010005 (2016).
5. R. W. Gerchberg and W. Saxton, "A practical algorithm for the determination of phase from image and diffraction plane pictures," Optik **35**, 237 (1971).
6. P. Zhou, Y. Li, S. Liu, and Y. Su, "Dynamic compensatory Gerchberg–Saxton algorithm for multiple-plane reconstruction in holographic displays," Opt. Express **27**, 8958 (2019).
7. P. Sun, S. Chang, S. Liu, X. Tao, C. Wang, and Z. Zheng, "Holographic near-eye display system based on double-convergence light Gerchberg–Saxton algorithm," Opt. Express **26**, 10140 (2018).
8. E. Buckley, "70.2: invited paper: holographic laser projection technology," SID Symp. Dig. Tech. Pap. **39**, 1074 (2008).
9. S. Jiao, D. Zhang, C. Zhang, Y. Gao, T. Lei, and X. Yuan, "Complex-amplitude holographic projection with a digital micromirror device (DMD) and error diffusion algorithm," IEEE J. Sel. Top. Quantum Electron. **26**, 19679194 (2020).
10. H. Pang, J. Wang, M. Zhang, A. Cao, L. Shi, and Q. Deng, "Non-iterative phase-only Fourier hologram generation with high image quality," Opt. Express **25**, 14323 (2017).
11. T. Shimobaba and T. Ito, *Computer Holography: Acceleration Algorithms and Hardware Implementations* (CRC Press, 2019).
12. P. W. M. Tsang and T. C. Poon, "Data-embedded-error-diffusion hologram (Invited Paper)," Chin. Opt. Lett. **12**, 060017 (2014).
13. R. Floyd and L. Steinberg, in *Adaptive Algorithm for Spatial Greyscale* (The Society for Information Display, 1976), Vol. **17**, p. 75.
14. R. Hauck and O. Bryngdahl, "Computer-generated holograms with pulse-density modulation," J. Opt. Soc. Am. A **1**, 5 (1984).
15. R. Eschbach, "Comparison of error diffusion methods for computer-generated holograms," Appl. Opt. **30**, 3702 (1991).
16. S. Weissbach, F. Wyrowski, and O. Bryngdahl, "Quantization noise in pulse density modulated holograms," Opt. Commun. **67**, 167 (1988).
17. P. W. Tsang and T. C. Poon, "Novel method for converting digital Fresnel hologram to phase-only hologram based on bidirectional error diffusion," Opt. Express **21**, 23680 (2013).
18. P. W. M. Tsang, A. S. M. Jiao, and T. C. Poon, "Fast conversion of digital Fresnel hologram to phase-only hologram based on localized error diffusion and redistribution," Opt. Express **22**, 5060 (2014).
19. G. Yang, S. Jiao, J. P. Liu, T. Lei, and X. Yuan, "Error diffusion method with optimized weighting coefficients for binary hologram generation," Appl. Opt. **58**, 5547 (2019).
20. Y. Zhao, L. Cao, H. Zhang, D. Kong, and G. Jin, "Accurate calculation of computer-generated holograms using angular-spectrum layer-oriented method," Opt. Express **23**, 25440 (2015).